Published in *J. Low Temp. Phys.* **150**, 394-401 (2008).

Journal of Low Temperature Physics manuscript No.
(will be inserted by the editor)

P. V. E. McClintock[1], V. B. Efimov[1,2],
A. N. Ganshin[1], G. V. Kolmakov[1,2],
and L. P. Mezhov-Deglin[2]

Turbulence of Second Sound Waves in Superfluid ^{4}He: Effect of Low-Frequency Resonant Perturbations

October 16, 2007

Keywords Wave turbulence, superfluid ^{4}He, second sound, energy cascade

Abstract We report the results of investigations of acoustic turbulence in a system of nonlinear second sound waves in a high-quality resonator filled with superfluid ^{4}He. It was observed that subharmonics of a periodic driving force applied to the system may be generated via a parametric instability. We find that application of an additional low-frequency pumping to the turbulent system results in the generation of waves at combination frequencies of the driving forces and also leads to substantial changes in the energy spectrum of the acoustic oscillations.

PACS Numbers: 67.40.Pm; 67.60.Fp.

1 INTRODUCTION

Second sound (a temperature-entropy wave) is a macroscopic quantum effect that arises in superfluids and perfect crystals[1,2]. The properties of second sound in He-II have been studied extensively, both experimentally and theoretically over many years. More recently, attention has been focused on the nonlinear acoustic properties of He-II[3,4,5]. It is known[1,2,6,7] that second sound is characterised by strong nonlinear properties. As a result of this nonlinearity, a propagating roton second sound pulse even of the quite small amplitude $\delta T \sim 1$ mK transforms into a shock wave over a relatively small distance $L \sim 1$ cm from the source[8].

The velocity u_2 of second sound depends on its amplitude and, to a first approximation, can be written as

$$u_2 = u_{20}(1 + \alpha \delta T) \quad (1)$$

1:Department of Physics, Lancaster University, Lancaster, LA1 4YB, UK

2:Institute of Solid State Physics RAS, 142432, Chernogolovka, Russia

where u_{20} is the wave velocity at negligibly small amplitude, δT is the wave amplitude in temperature T,

$$\alpha = \frac{\partial}{\partial T} \ln \left(u_{20}^3 \frac{C}{T} \right),$$

is the nonlinearity coefficient of second sound, and C is the heat capacity per unit mass of liquid helium at constant pressure.

The nonlinearity coefficient α may be either positive or negative, depending on the temperature and pressure [1,7]. Under the saturated vapour pressure, in the region of roton second sound (i.e. at $T > 0.9$ K) α is positive ($\alpha > 0$) for $T < T_\alpha = 1.88$ K, just like the nonlinearity coefficient of conventional sound waves in ordinary media. However, it is negative ($\alpha < 0$) in the range $T_\alpha < T < T_\lambda$. Here $T_\lambda = 2.176$ K is the temperature of the superfluid-to-normal (He-II to He-I) transition under the saturated vapour pressure. At $T = T_\alpha$, α passes through zero.

Second sound in He II within a high-Q resonator was recently used for an experimental study of acoustic or Burgers turbulence (BT) in a system of nonlinear sound waves [9]. Note that this turbulent state is radically different from quantum turbulence [10] (QT) in He II because the density of quantised vortices is close to zero. Furthermore, the motions of both the normal and superfluid components can be considered as being to a first approximation potential. BT has been at the focus of numerous investigations during the last few decades in view of its many important applications in engineering and fundamental science [11,12,13].

There are huge advantages in the use of roton second sound waves for the study of BT, including: the possibility of adjusting the nonlinearity coefficient of the second sound simply by changing the bath temperature, thus enabling one to study both nearly linear, and strongly nonlinear, waves while using exactly the same experimental techniques; the excellent time-resolution of the measurements due to the relatively small velocity of the second sound $u_{20} \leq 20$ m/s; and the ease with which the spectral characteristics of the driving force can be adjusted by changing the electrical signal applied to the heater used to generate the second sound.

It has been established [9] that a steady-state Kolmogorov-like wave energy cascade of acoustic turbulence can be formed in He II. It involves a flux of energy through the spectral range towards high frequencies, and arises when a periodic driving force of sufficiently high amplitude is applied at one of the resonant frequencies of the cavity. There is a smooth crossover in the system of second sound waves from the nearly linear regime at low driving amplitudes, to a nonlinear regime and, further, to developed turbulence at high driving amplitudes.

Here we demonstrate that acoustic waves with frequency *lower* than the driving frequency can also be generated due to nonlinearity. We report also the initial results of a study of the influence of an additional low-frequency periodic driving force on the steady-state turbulent energy distribution. We find that the application of a weak low-frequency perturbation to the turbulent system leads to the excitation of additional degrees of freedom – standing waves with frequencies equal to combinations of the main and additional driving frequencies. A redistribution of wave energy between the newly excited states leads to a decrease in the amplitudes of the nonlinearly generated waves in the high-frequency domain of the spectrum. We comment that turbulence “damping” on switching on the additional

energy input at low frequencies may be useful, for example in the control[14] of turbulence.

2 RESULTS AND DISCUSSION

2.1 Experimental Techniques

The experimental arrangements were similar to those used earlier[9] for the study of acoustic turbulence excited by a periodic driving force. We use a thin-film heater to generate the second sound, and a thin-film thermometer (a superconducting bolometer) as a detector. Use of a high-Q resonator enables us to create nonlinear second sound standing waves of high amplitude with only small heat production at the source. The wave amplitude δT can be changed from 0.05 mK up to a few mK. The resonator was formed by a cylindrical quartz tube of length $L = 7$ cm and inner diameter $D = 1.5$ cm. The film heater and bolometer were deposited on the surfaces of flat glass plates capping the ends of the tube. The measurements reported below were conducted under the saturated vapour pressure at $T = 2.08$ K where $\alpha \approx -7.6$ K^{-1}. The Q-factor of the resonator, determined from the widths of longitudinal resonances at small heat flux densities, was $Q \sim 1000$ for resonance numbers $p \leq 10$ and $Q \sim 3000$ for $30 < p < 100$.

In the present experiments, the heater could be driven by either or both of two external sinusoidal voltage generators in the frequency range between 0.1 and 100 kHz. When driving simultaneously at two frequencies the voltage applied to the heater was equal to

$$U(t) = U_1 \cos(\omega_1 t + \varphi_1) + U_2 \cos(\omega_2 t + \varphi_2). \quad (2)$$

The heat flux density emitted by the heater is proportional to the square of the voltage $U(t)$ applied to the heater,

$$W(t) = U^2(t)/RS, \quad (3)$$

where R and S are resistance and area of the heater. In the measurements reported below we applied a low-frequency driving force with $\omega_2 < \omega_1$ and $U_2 < U_1$. In order to drive at a single frequency ω_1, the driving voltage U_2 was set to zero, in which case only a standing wave of frequency $\omega_{d1} = 2\omega_1$ was excited.

If U_1 and U_2 are both nonzero then, in accordance with Eqs. 2 and 3, the frequencies of the excited second sound standing waves are equal to $\omega_{d1} = 2\omega_1$, $\omega_{d2} = 2\omega_2$, and $\omega_{d3,4} = \omega_1 \pm \omega_2$. Two types of measurements were conducted in the latter case. In each of them the main driving frequency ω_{d1} was always set equal to one of the longitudinal resonant frequencies of the cavity. In measurements of the first type second sound waves were excited by pumping effectively at the single frequency ω_{d1}: the additional driving frequency ω_{d2} was set far from any resonant frequency (typically, $\omega_{d2} \sim 1$ Hz), and, hence, the amplitudes of the second sound waves excited at the additional frequencies ω_{d2}, ω_{d3} and ω_{d4} were negligibly small due to high quality of the resonator. In measurements of the second type, the frequency ω_{d2} was set equal to some resonant frequency of the cavity. In this case second sound waves were excited simultaneously at four resonant frequencies ω_{d1}, ω_{d2}, ω_{d3} and ω_{d4}. In both cases the bolometer signal $A(t)$ was

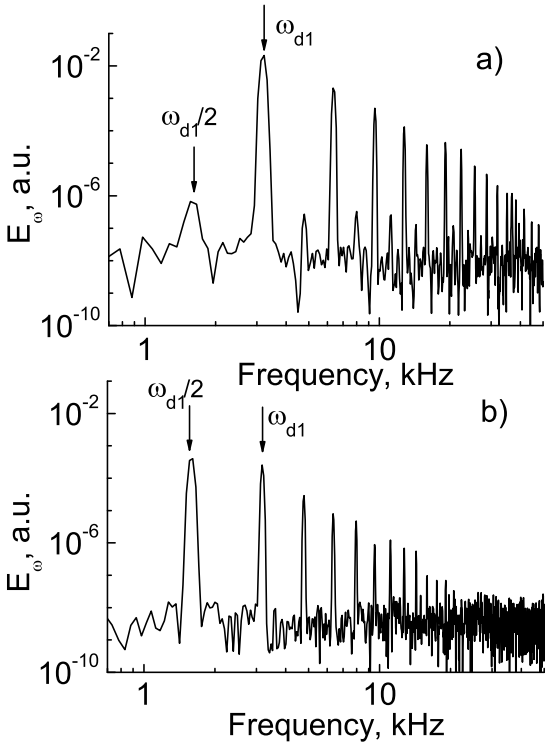

Fig. 1 Energy spectra of standing second sound waves measured at $T = 2.08$ K when driving at a single frequency of the 32nd resonance. The ac heat flux density was $W = 5.4$ W/cm^2 (a) and 42.1 W/cm^2 (b).

recorded and stored in computer memory. The second sound distribution over frequency was Fourier-analysed and the steady-state energy spectra were computed as

$$E_\omega = \text{const} \times |A_\omega|^2, \tag{4}$$

where A_ω is the time Fourier transform of the measured signal $A(t)$. We now present the results of these measurements in Sec. 2.2.

2.2 Experimental Observations

Figure 1 shows the spectra of standing second sound waves measured when driving at frequency of the 32nd resonance, $\omega_{d1}/2\pi = 3180$ Hz. In this measurement the additional driving voltage was $U_2 = 0$. The ac heat flux density was $W = 5.4$ W/cm^2 (plot (a)) and 42.1 W/cm^2 (plot (b)). The temperature of the helium bath was $T = 2.08$ K.

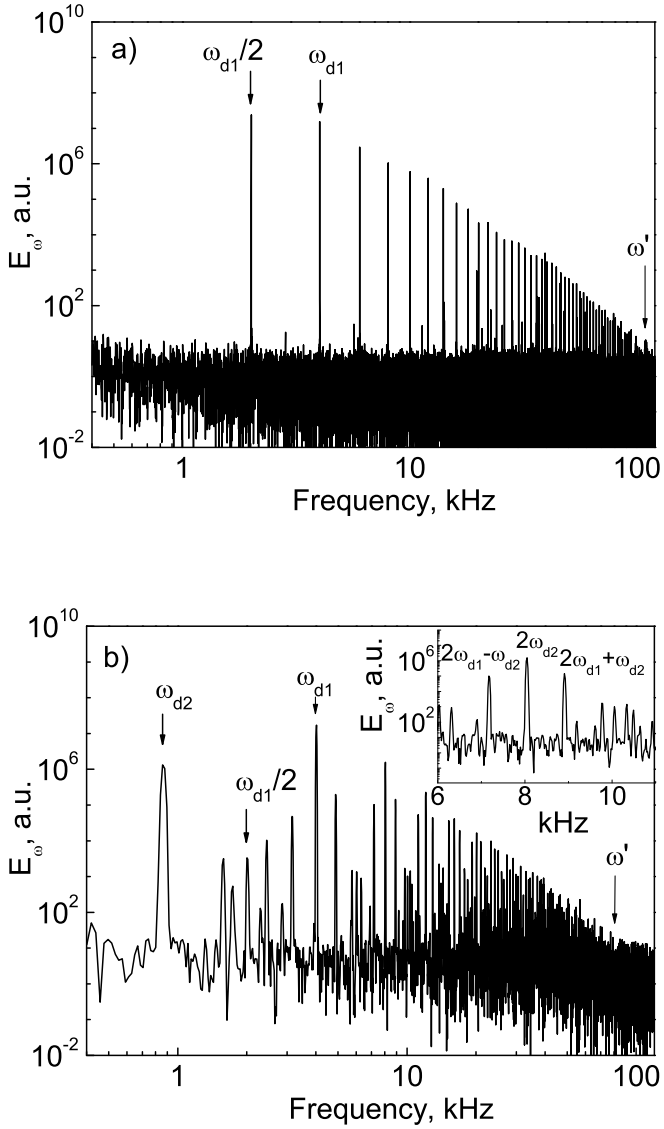

Fig. 2 Energy spectra of standing second sound waves measured at $T = 2.08$ K when driving at a single frequency of the 40th resonance (a) and simultaneously at two frequencies on the 9th and 40th resonances (b). The main driving frequency is $\omega_{d1}/2\pi = 4020.6$ Hz; the additional driving frequency is $\omega_{d2}/2\pi = 858.3$ Hz. The inset at the plate (b) shows an enlarged part of the spectrum near the 2nd harmonic of ω_{d1} in semi-log scale.

It is seen in Fig. 1(a) that spectral peaks are created at frequency ω_{d1} and its harmonics, similarly to our earlier observation[9]. Formation of the spectrum is attributable to a cascade transfer of wave energy through the frequency scales due to nonlinearity, thus establishing an energy flux in K-space directed from the driving frequency towards the high-frequency domain, and, hence, an acoustic turbulent state in the system of second sound waves (see Refs.[11,12,15] for general theory). At such a small ac heat flux density the amplitude of the wave of frequency equal to half the driving frequency, $\omega_{d1}/2 = \omega_1$, is negligibly small and is comparable with the amplitude of electrical noise.

At high driving voltage, however, formation of a peak at the frequency equal to *half* the driving frequency $\omega_{d1}/2$ is clearly seen in Fig. 1(b). Its amplitude is of the same order as the amplitude of fundamental peak at ω_{d1}. Generation of this subharmonic is probably caused by nonlinear three-wave processes in which a wave of frequency ω_{d1} decays into two waves with frequencies $\omega_{d1}/2$ due to a parametric instability[11], *i.e.* by the nonlinear process opposite to confluence of two waves, which causes generation of high frequency harmonics. We found that the peak at frequency $\omega_{d1}/2$ was *not* observed when driving at frequencies of the nearest resonances with odd resonant numbers (31st, *etc*), that supports our inference. As mentioned earlier[9], excitation of a subharmonic of the driving frequency leads to an effective decrease of the inertial interval of frequencies where the turbulent spectrum is established.

Figure 2 presents some typical experimental results obtained when driving simultaneously at two frequencies (U_1 and U_2 both being nonzero). The ac heat flux density at the main driving frequency ω_{d1} was $W_1 = 21.5$ mW/cm^2, and the ac heat flux densities at the additional driving frequencies were $W_2 = 0.16\,W_1 = 3.4$ mW/cm^2 at the frequency ω_{d2} and $W_{3,4} = 0.8\,W_1 = 17.2$ mW/cm^2 at the frequencies ω_{d3} and ω_{d4}.

Fig. 2(a) shows the steady-state energy spectrum of second sound waves measured when driving effectively at a single frequency of the 40th resonance (measurements of the first type). It is evident from Fig. 2(a) that the fundamental spectral peak lies at the driving frequency ω_{d1}, and a subharmonic peak of comparable amplitude lies at half the driving frequency $\omega_{d1}/2$. The high-frequency peaks appear at harmonics of both the fundamental driving frequency and its subharmonics, $\omega_n = n \times \omega_{d1}/2$ with $n = 1,2,3\ldots$.

Fig. 2(b) shows the spectrum obtained in a measurement of the second type, when the driving frequency ω_{d2} was set equal to the 9th resonant frequency, in addition to the main drive. The frequencies $\omega_{d3,4}$ lay far from any longitudinal resonance of the cavity, and waves with these frequencies were not excited. It is clearly seen that additional peaks are formed at *combination* frequencies $\omega_{mn} = m \times \omega_{d1} + n \times \omega_{d2}$ (where n and m are integer numbers) along with harmonics of the main driving frequency. These peaks are evidently formed through nonlinear interactions between the waves at the main and additional driving frequencies. This phenomenon is similar to the generation of combination frequencies during the propagation of light through a nonlinear optical medium[16]. Formation of Stokes and anti-Stokes satellites of the 2nd harmonics of the main drive at frequencies $\omega = 2\omega_{d1} \pm \omega_{d2}$, corresponding to "absorption" and "emission" of the second sound waves with frequency ω_{d2} due to nonlinearity, is clearly seen in the spectrum shown in the inset of Fig. 2(b).

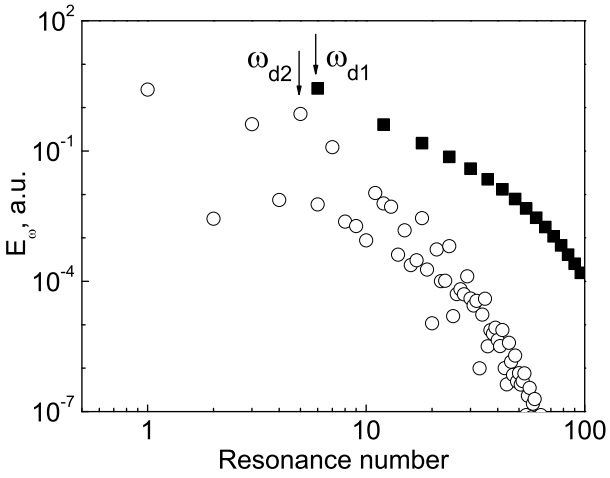

Fig. 3 Calculated energy distributions of nonlinear second sound waves. Solid squares: driving at the 6th resonant frequency of the resonator; open circles: driving simultaneously at the 5th and 6th resonant frequencies. The low-frequency ac heat flux density W_2 is equal to $0.1\times$ the ac heat flux density W_1 at the main driving frequency.

It is evident from Fig. 2 that the inertial interval of frequencies is reduced by application of the additional driving force to the system: the characteristic frequency $\omega'/2\pi$, at which the peaks fall below the electrical noise level (~ 10 a.u.) is decreased from ~ 110 kHz in Fig. 2(a) to ~ 82 kHz in Fig. 2(b). Note that a very similar effect – reduction of the high-frequency oscillations by application of an additional low-frequency perturbation to a turbulent system – was recently observed in experiments with capillary waves on the surface of liquid hydrogen[17].

2.3 Numerical Calculations

To try to understand how the application of a low frequency perturbation affects the turbulent distribution, we have performed a numerical study of the dynamics of nonlinear second-sound waves within the high-Q resonator. The numerical technique was similar to that used earlier in studies of the formation of steady-state turbulent second sound spectra[9]. Figure 3 shows the calculated changes in the steady-state energy spectrum of second sound after switching on the low-frequency perturbation. We assumed that the main driving force is applied at the 6th resonant frequency and that the additional driving force is applied at the 5th resonant frequency. It is clearly evident that application of a small perturbation with $W_2 \sim 0.1W_1$ (i.e. not much different from the ratio of 0.16 used in the experiments) leads to the formation of waves with frequencies equal to combinations of the driving force frequencies and to a *substantial* reduction in wave amplitude at frequencies above the main driving frequency. Generation of waves with frequencies lower than ω_{d2}, *i.e.* the 1st, 2nd, *etc*, resonances, as seen in Fig. 3 (open

circles), is caused by excitation of combination frequencies of the main and additional drive, $\omega_{d1} - \omega_{d2}$ and its harmonics. Numerical estimation shows that the total wave energy $E_{\rm hf}$ contained in the high frequency domain (waves with resonance numbers $p \geq 7$) is decreased by $\sim 4\times$ after the additional driving force is applied. The reason for the damping of the high-frequency turbulent cascade is probably an outflow of energy from the high-frequency spectral domain towards the low-frequency energy-containing domain after application of the perturbation. We plan to study this phenomenon in detail in the near future.

3 CONCLUSIONS

We have shown in experiments with a turbulent system of second sound waves in a high-Q resonator filled with superfluid helium that acoustic waves with frequency lower than the driving frequency may be generated due to nonlinearity: a sound wave with frequency equal to half the driving frequency (subharmonic of the driving frequency) may be excited at relatively large ac heat flux densities. We suppose that the subharmonic is generated through a decay instability of the wave excited by an external drive. We have also found in both experiments and numerical calculations that application of an additional low frequency driving force to a turbulent system of second sound waves results in the excitation of additional acoustic oscillations with frequencies equal to combination frequencies of the main and additional driving forces. The amplitudes of the second sound waves in the high frequency spectral domain are decreased when the additional driving force is applied. Suppression of the turbulent cascade in the high-frequency domain is probably caused by redistribution of the wave energy among newly excited states in the low-frequency energy-containing region.

Acknowledgements We are grateful to V. E. Zakharov, E. A. Kuznetsov, A. A. Levchenko and M. Yu. Brazhnikov for valuable discussions. The investigations were supported by the Russian Foundation for Basic Research project Nos. 07-02-00728 and 06-02-17253, by the Presidium of the Russian Academy of Sciences in framework of the programmes “Quantum Macrophysics” and “Mathematical Methods in Nonlinear Dynamics”, and by the Engineering and Physical Sciences Research Council (U.K.).

References

1. I. M. Khalatnikov, *An Introduction to the Theory of Superfluidity* (Benjamin, New York, 1965).
2. S. J. Putterman, *Superfluid Hydrodynamics* (North-Holland Publishing Corp., Amsterdam, 1974).
3. A. Yu. Iznankin and L. P. Mezhov-Deglin, *Sov. Phys. JETP* **57**, 801 (1983).
4. S. K. Nemirovsky, *Usp. Fiz. Nauk* **160**, 51 (1990).
5. L. S. Goldner, G. Ahlers, and R. Mehrotra, *Phys. Rev.* **43**, 12861 (1991).
6. D. V. Osborne, *Proc. Phys. Soc.* (London) **A64**, 114 (1951).
7. A. J. Dessler and W. H. Fairbank, *Phys. Rev.* **104**, 6 (1956).
8. G. V. Kolmakov, V. B. Efimov, A. N. Ganshin, P. V. E. McClintock, and L. P. Mezhov-Deglin, *Low Temp. Phys.* **32**, 999 (2006).

9. G. V. Kolmakov, V. B. Efimov, A. N. Ganshin, P. V. E. McClintock, and L. P. Mezhov-Deglin, *Phys. Rev. Lett.* **97**, 155301 (2006).
10. W. F. Vinen, *J. Low Temp. Phys.* 145, 7 (2006).
11. V. E. Zakharov, G. Falkovich, and V. S. L'vov, *Kolmogorov Spectra of Turbulence I* (Springer, Berlin, 1992).
12. G. Falkovich and M. Meyer, *Phys. Rev.* E **54**, 4431 (1996).
13. S. N. Gurbatov, V. V. Kurin, L. M. Kustov, and N. V. Pronchatov-Rubtsov, *Acoust. Phys.* **51**, 152 (2005).
14. *Transition and Turbulence Control*, M. Gad-el-Hak and H. M. Tsai, eds., Lecture Notes Series, Vol. 8 (Institute for Mathematical Sciences, National University of Singapore, 2005).
15. E. A. Kuznetsov, *JETP Lett.* **80**, 83 (204).
16. P. A. Franken, A. E. Hill, C. W. Peters, and G. Weinreich, *Phys. Rev. Lett.* **7**, 118 (1961).
17. M. Yu. Brazhnikov, G. V. Kolmakov, A. A. Levchenko, and L. P. Mezhov-Deglin, *JETP Lett.* **82**, 565 (2005).